THE JOURNAL OF CHEMICAL PHYSICS **137**, 084706 (2012)

Vapor-liquid interfacial properties of rigid-linear Lennard-Jones chains

F. J. Blas,[1,a)] A. Ignacio Moreno-Ventas Bravo,[2] J. M. Míguez,[3] M. M. Piñeiro,[3] and L. G. MacDowell[4]
[1]*Departamento de Física Aplicada, Universidad de Huelva, 21071, Huelva, Spain*
[2]*Departamento de Geología, Facultad de Ciencias Experimentales, Universidad de Huelva, 21071 Huelva, Spain*
[3]*Departamento de Física Aplicada, Universidade de Vigo, 36310 Vigo, Spain*
[4]*Departamento de Química Física, Facultad de Ciencias Químicas, Universidad Complutense, Madrid 28040, Spain*

(Received 17 June 2012; accepted 1 August 2012; published online 30 August 2012)

We have obtained the interfacial properties of short rigid-linear chains formed from tangentially bonded Lennard-Jones monomeric units from direct simulation of the vapour-liquid interface. The full long-range tails of the potential are accounted for by means of an improved version of the inhomogeneous long-range corrections of Janeček [J. Phys. Chem. B **110**, 6264–6269 (2006)] proposed recently by MacDowell and Blas [J. Chem. Phys. **131**, 074705 (2009)] valid for spherical as well as for rigid and flexible molecular systems. Three different model systems comprising of 3, 4, and 5 monomers per molecule are considered. The simulations are performed in the canonical ensemble, and the vapor-liquid interfacial tension is evaluated using the test-area method. In addition to the surface tension, we also obtain density profiles, coexistence densities, critical temperature and density, and interfacial thickness as functions of temperature, paying particular attention to the effect of the chain length and rigidity on these properties. According to our results, the main effect of increasing the chain length (at fixed temperature) is to sharpen the vapor-liquid interface and to increase the width of the biphasic coexistence region. As a result, the interfacial thickness decreases and the surface tension increases as the molecular chains get longer. The surface tension has been scaled by critical properties and represented as a function of the difference between coexistence densities relative to the critical density. © *2012 American Institute of Physics*. [http://dx.doi.org/10.1063/1.4746120]

I. INTRODUCTION

The knowledge of interfacial properties plays a key role, not only in many scientific fields such as nucleation or dynamics of phase transitions, but also in a great number of practical and industrial applications, attracting the attention from simulators of the liquid community over the last years. From the theoretical and practical point of view, the surface tension is obviously the most important and challenging property to be determined and predicted in the context of inhomogeneous systems.[1–3] Despite the great number of studies, especially in the area of computer simulation, the calculation of surface tension remains a subtle problem due to different reasons, including the ambiguity in the definition of the pressure tensor, the finite size effects due to capillary waves, or the difficulty for the calculation of the long-range corrections (LRCs) associated to intermolecular interactions.

From a microscopic point of view, interfacial problems can be studied using well-established statistical mechanics tools, and particularly, molecular simulation techniques, which are routinely used to examine inhomogeneous systems. Computer simulation methods have experienced a great development in this field during last years, especially on new techniques for the determination of fluid-fluid interfacial tension. The standard methodology for calculating the interfacial tension involves the mechanical route through the determination of the normal and tangential pressure tensor profiles using the virial according to the recipes of Irving and Kirkwood,[4] and Harasima,[5] among others. A useful and recent revision of the theoretical background of the methods of Irving and Kirkwood and Harasima can be found in the work of Varnik *et al.*[6]

Alternatively, more effective, and elegant methods based on the thermodynamic definition of surface tension have been introduced, developed, and used during the last decade, including the expanded ensemble[7] and wandering interface method,[8] or perturbative procedures such as the test-area (TA) technique[9] or the determination of the macroscopic components of the pressure tensor (using virtual changes to evaluate the corresponding Boltzmann factor, as the methodology proposed by de Miguel and Jackson[10,11] or Brumby *et al.*[12]). These methods are becoming very popular and are being used routinely to determine the vapour-liquid interfacial properties of Lennard-Jones (LJ),[13–15] several models of water,[16,17] the Mie potential[18] or binary mixtures,[19–21] among others.

The methodology to account for the interactions beyond cutoff in systems that exhibit a planar vapour-liquid interface, and in general, any inhomogeneity with planar symmetry, has been until recently a difficult problem to solve. Different authors have contributed to the establishment of appropriate and standard LRCs, including Blokhius,[22] Mecke,[23,24] Daoulas,[25] Guo and Lu,[26] and finally, Janeček,[27,28] and the

a)Electronic mail: felipe@uhu.es.

recent improved methods proposed by MacDowell and Blas[14] and de Gregorio *et al.*[29]

As a consequence of the intensive and deep development of the new methods and techniques in molecular simulation, a great number of studies for determining the interfacial properties of molecular systems, with special emphasis on chain-like molecules and its interfacial tension, have been carried out lately.[30,31] Chain-like molecules are substances formed from monomeric units with a certain degree of flexibility, and n-alkanes molecules and their isomers lie in this general set of molecules. All of them exhibit intramolecular flexibility governed by bending and torsional potentials, that determine the molecular configurations the chains can adopt without overlaps.

From a formal point of view, n-alkanes exhibit an intermediate behaviour between those shown by two well-known model systems, i.e., the fully-flexible[13,14,32–35] and rigid-linear LJ chain models.[36] The fully-flexible chain-like system has neither bending nor torsional potentials between the monomers in a chain. Therefore, there is no energetic penalty when the monomers of the chains adopt a close packed structure at high densities. On the contrary, in the rigid-linear chain model the bond length, bond angles, and internal degrees of freedom are fixed. As a consequence of this, both models exhibit completely different phase diagrams, as demonstrated several years ago by Galindo *et al.*[36] Apparently, the vapour-liquid phase behaviour of both models seems to exhibit small differences: rigid-linear LJ chains exhibit vapour-liquid coexistence curves wider and higher critical temperatures than the corresponding to fully-flexible chains. In addition to that, a clear stabilization of the solid phase with respect to the fluid is seen for increasing chain lengths in the case of rigid-linear LJ chains, contrary to that exhibited by fully-flexible LJ molecules. As a consequence of this, a marked increase of the triple-point temperature is observed, whereas the triple-point temperature of fully-flexible LJ chains is practically independent of the chain length. In summary, as a result of the stabilization of the solid phase, the fluid range (characterized by the ratio of triple temperature to critical temperature) decreases for increasing chain length, and it is predicted to disappear for chains with more than six LJ monomers.[36] This is in marked contrast with the phase behaviour of fully-flexible LJ chains, which is dominated by the vapour-liquid coexistence. In fact, the phase diagram of rigid-linear LJ chains is probably much more different than that of fully-flexible LJ chains due to the presence of liquid crystalline mesophases. This point was previously indicated by Galindo *et al.*[36] In addition to that, a similar model, the rigid-linear hard-sphere chain-like model considered by Vega *et al.*[37] several years ago, exhibits liquid crystalline phases for chain lengths equal or larger than five segments, including isotropic, nematic, and smectic, a phase between the isotropic liquid and solid phases. Currently, Blas and del Río[38] are investigating the phase diagram of rigid-linear LJ chains formed from 6–9 monomeric units. Preliminary results indicate the existence of intermediate liquid crystal phases (nematic). This corroborates the previous hypothesis of Galindo *et al.*[36] on the existence of intermediate (liquid crystal) mesophases of rigid-linear LJ chains.

It is clear from the ensuing discussion that a first attempt to determine the phase diagram and other thermodynamic properties of rigid molecules should first involve a careful study of the isotropic liquid phases. During the last years, there has been an increasing number of studies to determine the interfacial properties of very realistic chain-like systems modelling n-alkanes and some of their isomers.[39–41] However, only a reduced number of works have been dedicated to determine the interfacial properties of simpler chain-like models. These systems, although more simplified, are able to provide important information on how microscopic parameters determine the macroscopic interfacial properties. In particular, the study and comparison of the phase diagram and interfacial properties of two simple models with different molecular architecture, such as fully-flexible and rigid-linear chain-like systems, would provide a valuable information on how the internal degrees of freedom (flexibility) control the interfacial properties of chain-like systems.

The main goal of this work is to study the vapour-liquid interfacial properties of short rigid-linear LJ chains. Here, we concentrate in short chain-like systems that only exhibit isotropic fluid but not liquid crystalline phases, apart from the corresponding stable solid phases. In particular, we consider the effect of temperature and chain length on the vapour-liquid coexistence curve, interfacial thickness, and surface tension. In addition to that, we extend the improved method of Janeček to account for LRCs, proposed recently by MacDowell and Blas, to deal with rigid molecules. This technique allows to determine the thermodynamic, including phase equilibria, and interfacial properties of rigid-linear LJ chains interacting through the full potential. In a recent paper,[42] it has been shown that the use of this formal scheme to account for the LJ LRCs represents a relevant contribution to the interfacial properties of systems that interact through this intermolecular potential, which are not adequately described from a quantitative point of view by a simple truncation of the potential, even for long cut-off radius.

The rest of the paper is organized as follows. In Sec. II we consider an improved method for determining the long-range corrections of inhomogeneous chain-like systems. The molecular model and the simulation details of this work are presented in Sec. III. Results obtained are discussed in Sec. IV. Finally, in Sec. V we present the main conclusions.

II. EFFECTIVE LONG-RANGE PAIRWISE POTENTIAL FOR MOLECULAR SYSTEMS

In 2006, Janeček[27] proposed a new methodology for calculating LRC to the energy in systems that interact through spherically symmetric intermolecular potentials. This procedure allows to treat in a simple way the truncation of the intermolecular energy of systems that exhibit planar interfaces. More recently, MacDowell and Blas[14] have demonstrated that the Janeček's procedure can be rewritten into an effective long-range pair potential plus a self term that allows for a fast, easy, and elegant implementation of the method. Since the original and improved methodologies have been introduced

elsewhere,[14,27,28] we only account here for the most important details of the current version for spherical molecules. In particular, we focus on the methodology for chain-like molecules and discuss the particular expressions for linear tangent chains.

Consider a system of N spherical molecules contained in a volume V that interact through a pairwise intermolecular potential. The total intermolecular potential energy can be written as

$$U = \frac{1}{2}\sum_{i=1}^{N}\sum_{\substack{j=1\\(j\neq i)}}^{N} u(r_{ij}) = \frac{1}{2}\sum_{i=1}^{N} U_i, \tag{1}$$

where $u(r_{ij})$ is the intermolecular potential between particles i and j, that depends on the distance between the centres of molecules $r_{ij} \equiv |\mathbf{r}_i - \mathbf{r}_j|$, and U_i is the potential energy of molecule i due to the interactions with all molecules of the system. During a simulation, the potential energy of a particle is usually split into two contributions: one arising from the interaction of molecule i with all molecules inside a sphere of radius $r_c^{(i)}$ centered at this molecule, and a second term that corresponds to the interaction between the molecule i and the rest of molecules forming the system (i.e., all the molecules located outside the cut-off sphere). The potential energy of a molecule i can be then written as

$$U_i = \sum_{j\in r_c^{(i)}} u(r_{ij}) + U_i^{\mathrm{LRC}}, \tag{2}$$

where $r_c^{(i)}$ is the so-called cut-off distance of particle i, the notation $j \in r_c^{(i)}$ denotes all the particles j located inside the cut-off sphere centered at the position of particle i, and U_i^{LRC} represents the intermolecular interactions between particle i and the rest of the system due to LRC. Note that $r_c^{(i)} \equiv r_c$ since all molecules have the same cut-off distance.

In the original Janeček's methodology, the simulation box is divided into strips parallel to the xy-plane (and to the planar interface) of width Δz, in such a way that the number density of the system $\rho(z)$ is considered to be approximately constant inside of each of them. Here we have chosen arbitrarily the z-axis as the direction along which the simulation box exhibits its inhomogeneity, consisting in a planar interface. If one assumes that the pair correlation function between two particles separated beyond the cut-off distance is equal to one, i.e., the distribution of particles separated a distance $r_{ij} \geq r_c$ is uniform, the intermolecular potential of a particle i located at position z_i associated to the long-range interaction with the rest of the system is given by[27]

$$U_i^{\mathrm{LRC}}(z_i) = \sum_{k=1}^{n_s} w(|z_i - z_k|)\rho(z_k)\Delta z, \tag{3}$$

where $\rho(z_k)$ is the density of the system in the slab of width Δz and centered at z_k, the index k runs for all the n_s slabs in which the simulation box is divided along the z-axis, and $w(|z_i - z_k|)$ accounts for the intermolecular interactions due to the LRC between a particle i at z_i and all the particles located inside the slab centered at z_k. The particular expression for $w(|z_i - z_j|)$ depends on the election of the intermolecular potential of the system. In the original Janeček's method, applicable for molecules interacting through the Lennard-Jones intermolecular potential, the function $w(z)$ is given by

$$w(z) = \begin{cases} 4\pi\epsilon\sigma^2\left[\frac{1}{5}\left(\frac{\sigma}{r_c}\right)^{10} - \frac{1}{2}\left(\frac{\sigma}{r_c}\right)^{4}\right], & z < r_c \\ 4\pi\epsilon\sigma^2\left[\frac{1}{5}\left(\frac{\sigma}{z}\right)^{10} - \frac{1}{2}\left(\frac{\sigma}{z}\right)^{4}\right], & z > r_c. \end{cases} \tag{4}$$

The total energy arising from the LRCs is given as a sum over individual contributions, with a factor of 1/2 not to include mutual interactions twice,

$$U^{\mathrm{LRC}} = \frac{1}{2}\sum_{i=1}^{N} U_i^{\mathrm{LRC}}(z_i). \tag{5}$$

Equations (3)–(5) constitute the original Janeček's method for estimating the intermolecular interactions of the system due to LRCs. Although this method allows to calculate very accurately the LRCs of a Lennard-Jones system that exhibits a planar interface, it has several drawbacks. The most important one is the calculation of the density profile on the fly, i.e., it is necessary to have the instantaneous density profile every step for being used in Eq. (3) and hence, to be able to calculate the tail corrections at each Monte Carlo step. Unfortunately, this makes the procedure cumbersome, especially in the case of molecular fluids,[14] and also complicates the programming since the density profile must be updated each Monte Carlo step.

The improved methodology proposed recently by MacDowell and Blas,[14] simpler and more accurate, elegant, and easier to implement in a simulation code than the original one, assumes that Eq. (3) can be written more accurately as

$$U_i^{\mathrm{LRC}}(z_i) = \int_{-\infty}^{+\infty} w(|z_i - z|)\,\rho(z)\,dz. \tag{6}$$

The density profile of a system formed by N particles can be written formally as a summation of δ-Dirac distributions centered at the positions z_j, with $j = 1, \ldots, N$,

$$\rho(z) = \frac{1}{\mathcal{A}}\sum_{j=1}^{N}\delta(z - z_j), \tag{7}$$

where $\mathcal{A}$ is the interfacial area of the xy-plane of the system. Using Eq. (7) in Eq. (6), $U_i^{\mathrm{LRC}}(z_i)$ is given by

$$U_i^{\mathrm{LRC}}(z_i) = \frac{1}{\mathcal{A}}\sum_{j=1}^{N} w(|z_i - z_j|). \tag{8}$$

It is important to note that summation in Eq. (8) runs over all the values of the index j ($j = 1, \ldots, N$), and this also includes the case $j = i$.

The total intermolecular interaction energy arising from the LRCs, given by Eq. (5), is then expressed as

$$U^{\mathrm{LRC}} = \frac{1}{2\mathcal{A}} \sum_{i=1}^{N} \sum_{j=1}^{N} w(|z_i - z_j|). \tag{9}$$

The unrestricted summation over indexes i and j can be finally transformed into a sum of pairwise effective (integrated) intermolecular potential over all the pairs of molecules in the system and N self-energy terms as

$$U^{\mathrm{LRC}} = \frac{1}{\mathcal{A}} \sum_{i=1}^{N-1} \sum_{j=i+1}^{N} w(|z_i - z_j|) + \frac{1}{2\mathcal{A}} \sum_{i=1}^{N} w(0). \tag{10}$$

The expressions given by Eqs. (8) and (10) are the key relationships of the improved version proposed by MacDowell and Blas:[14] the interaction energy due to the LRCs are given by an effective pairwise intermolecular potential between all the particles forming the system.

The last term in Eq. (10), the self-energy contribution, is not a truly summation of self energy terms. In fact, the function $w(z)$ is not a real intermolecular potential between a pair of particles but an effective (integrated) potential. Each contribution $\frac{1}{\mathcal{A}} w(|z_i - z_j|)$ in Eq. (8) represents the intermolecular potential, due to the interactions between the particle i with all the particles located inside the slab centered at z_j due to the long-range interactions. Therefore, $w(0)$ represents the long-range intermolecular interactions between a molecule and the rest of molecules located inside the same slab but beyond the cut-off radius.

Now we present the extension of the methodology for the general case of systems of chain-like molecules formed by a number of monomeric units. We first formulate the extension for the most general case, including molecules with intermolecular and intramolecular interactions. The particular case of rigid-linear LJ chains, which corresponds to a system in which intramolecular interactions are constant and hence irrelevant, is also discussed in detail at the end of this section.

In the case of molecular systems, and particularly in molecules formed from monomeric segments, the interaction due to the LRCs between a given segment k of a molecule i and the rest of the system should have three different contributions according to the ensuing discussion: (a) an intermolecular contribution, $U^{\mathrm{LRC}}_{i,k,inter}$, to account for the LRCs between the segment k of the molecule i with all the segments of the rest of the chains forming the system, $j = 1, \ldots N$, with $j \neq i$; (b) an intramolecular contribution, $U^{\mathrm{LRC}}_{i,k,intra}$, accounting for the LRCs between the segment k of the molecule i and the rest of segments of the same chain i, $k' = 1, \ldots m$, with $k' \neq k$; and finally (c) a self-energy contribution, $U^{\mathrm{LRC}}_{i,k,self}$, which takes into account the interaction due to the LRCs associated to the self-energy term of the segment k. The total energy felt by the segment k of the molecule i, located at position $z_{i,k}$ can be written as

$$\begin{aligned} U^{\mathrm{LRC}}_{i,k}(z_{i,k}) &= U^{\mathrm{LRC}}_{i,k,inter}(z_{i,k}) + U^{\mathrm{LRC}}_{i,k,intra}(z_{i,k}) + U^{\mathrm{LRC}}_{i,k,self}(z_{i,k}) \\ &= \frac{1}{\mathcal{A}} \sum_{\substack{j=1 \\ (j\neq i)}}^{N} \sum_{k'=1}^{m} w(|z_{i,k} - z_{j,k'}|) \\ &\quad + \frac{1}{\mathcal{A}} \sum_{\substack{k'=1 \\ (k'\neq k)}}^{m} w(|z_{i,k} - z_{i,k'}|) + \frac{1}{\mathcal{A}} w(|z_{i,k} - z_{i,k}|) \\ &= \frac{1}{\mathcal{A}} \sum_{\substack{j=1 \\ (j\neq i)}}^{N} \sum_{k'=1}^{m} w(|z_{i,k} - z_{j,k'}|) \\ &\quad + \frac{1}{\mathcal{A}} \sum_{\substack{k'=1 \\ (k'\neq k)}}^{m} w(|z_{i,k} - z_{i,k'}|) + \frac{1}{\mathcal{A}} w(0). \end{aligned} \tag{11}$$

The total energy felt by the whole molecule i, due to the long-range interactions with all the molecules that form the system, can be written as

$$U^{\mathrm{LRC}}_{i} = U^{\mathrm{LRC}}_{i,inter} + U^{\mathrm{LRC}}_{i,intra} + U^{\mathrm{LRC}}_{i,self}. \tag{12}$$

The intermolecular potential energy between molecule i and the rest of molecules forming the system, due to the LRCs, can be written as

$$U^{\mathrm{LRC}}_{i,inter} = \frac{1}{\mathcal{A}} \sum_{\substack{j=1 \\ (j\neq i)}}^{N} \sum_{k=1}^{m} \sum_{k'=1}^{m} w(|z_{i,k} - z_{j,k'}|). \tag{13}$$

The energy corresponding to the intramolecular interactions associated to segments of molecule i is given by

$$U^{\mathrm{LRC}}_{i,intra} = \frac{1}{\mathcal{A}} \sum_{k=1}^{m-1} \sum_{k'=k+1}^{m} w(|z_{i,k} - z_{i,k'}|). \tag{14}$$

Note that Eq. (14) only takes into account the intramolecular interactions, associated to the LRC, i.e., all possible interactions between segments of molecule i.

And finally, the self-energy contribution to the potential energy of molecule i can be simply written as

$$U^{\mathrm{LRC}}_{i,self} = \frac{1}{\mathcal{A}} \sum_{k=1}^{m} w(0) \equiv \frac{1}{\mathcal{A}} m w(0). \tag{15}$$

The self-energy contribution associated to the long-range interactions given by Eq. (15) is only due to segments belonging to molecule i.

The total potential energy of a system of N molecules formed by m segments, due to the long-range interactions, is then calculated as

$$U^{\mathrm{LRC}} = U^{\mathrm{LRC}}_{inter} + U^{\mathrm{LRC}}_{intra} + U^{\mathrm{LRC}}_{self}. \tag{16}$$

The total intermolecular potential energy, due to the long-range interactions, is given by

$$U_{inter}^{\mathrm{LRC}} = \frac{1}{2}\sum_{i=1}^{N} U_{i,inter}^{\mathrm{LRC}} = \frac{1}{2\mathcal{A}}\sum_{i=1}^{N}\sum_{\substack{j=1\\(j\neq i)}}^{N}\sum_{k=1}^{m}\sum_{k'=1}^{m} w(|z_{i,k}-z_{i,k'}|)$$

$$= \frac{1}{\mathcal{A}}\sum_{i=1}^{N-1}\sum_{j=i+1}^{N}\sum_{k=1}^{m}\sum_{k'=1}^{m} w(|z_{i,k}-z_{j,k'}|), \quad (17)$$

where we have transformed the unrestricted summation over indexes i and j (with the exception of the case $i = j$ corresponding to intramolecular interactions) into a sum of pairwise effective (integrated) intermolecular potential over all the pair of molecules in the system, similarly to the case of spherical molecules (see Eq. (10)).

The total intramolecular potential energy due to the long-range interactions is given by

$$U_{intra}^{\mathrm{LRC}} = \sum_{i=1}^{N} U_{i,intra}^{\mathrm{LRC}} = \frac{1}{\mathcal{A}}\sum_{i=1}^{N}\sum_{k=1}^{m-1}\sum_{k'=k+1}^{m} w(|z_{i,k}-z_{i,k'}|). \quad (18)$$

Finally, the total self-energy potential energy due to the long-range interactions is written as

$$U_{self}^{\mathrm{LRC}} = \frac{1}{2}\sum_{i=1}^{N} U_{i,self}^{\mathrm{LRC}} = \frac{1}{2\mathcal{A}}\sum_{i=1}^{N}\sum_{k=1}^{m} w(0) \equiv \frac{1}{2\mathcal{A}}\sum_{i=1}^{N} m w(0)$$

$$\equiv \frac{1}{2\mathcal{A}} N m w(0). \quad (19)$$

Equations (12)–(19) represent the generalization of the improved version of MacDowell and Blas,[14] based on Janeček's method, for the inhomogeneous LRC of chain-like systems, including flexible and rigid molecules. Since in this work we are dealing with the case of rigid linear Lennard-Jones chains, the intramolecular potential energy is constant and set to zero. Consequently, the corresponding contribution due to the long-range interactions is also set equal to zero, i.e., $U_{intra}^{\mathrm{LRC}} = 0$. In this work, we calculate the total potential energy of molecule i associated to the LRC as

$$U_{i}^{\mathrm{LRC}} = \frac{1}{\mathcal{A}}\sum_{\substack{j=1\\(j\neq i)}}^{N}\sum_{k=1}^{m}\sum_{k'=1}^{m} w(|z_{i,k}-z_{j,k'}|) + \frac{1}{\mathcal{A}} m w(0), \quad (20)$$

and the corresponding total potential energy as

$$U^{\mathrm{LRC}} = \frac{1}{\mathcal{A}}\sum_{i=1}^{N-1}\sum_{j=i+1}^{N}\sum_{k=1}^{m}\sum_{k'=1}^{m} w(|z_{i,k}-z_{i,k'}|) + \frac{1}{2\mathcal{A}} N m w(0). \quad (21)$$

It is important to recall here that the intramolecular interactions (due to LRCs) for rigid-linear LJ chains, i.e., $U_{i,intra}^{\mathrm{LRC}}$ and U_{intra}^{LRC}, are strictly constant due to the rigidity of the chain and intramolecular constrains of the molecular model. However, this contribution must be taken into account when dealing with molecular systems that have intramolecular interactions, as in the case of fully-flexible LJ chains. Special care should be taken in the case of long-chain molecules in which monomeric units of the same chain separated by distances larger than r_c can interact, and consequently, the intramolecular LRC, $U_{i,intra}^{\mathrm{LRC}}$ and U_{i}^{LRC}, must be calculated.

This procedure provides several important advantages over the original method: (1) Eqs. (8) and (10), for the case of spherical fluids, and Eqs. (12)–(19) for molecular systems, correspond to the exact evaluation of the intermolecular interactions due to the LRCs. It is important to recall that the use of the original Janeček version of the method implies a discretization of the simulation box along the z-axis, which is in fact an approximation; (2) the improved procedure allows to evaluate U_{i}^{LRC} and U^{LRC} without the explicit calculation of the density profile on the fly, i.e., it is not necessary to update the density profile $\rho(z)$ each Monte Carlo step. Just to give an order of magnitude, if the simulation of the vapour-liquid interface of a Lennard-Jones system is equilibrated typically in 10^6 Monte Carlo cycles, and in each cycle we attempt to move N molecules ($N \sim 10^3$ molecules), the density profile of the system should be updates 10^9 times along the equilibration stage; (3) finally, the implementation of the method is straightforward. If one has a standard Monte Carlo code in the canonical ensemble, the only change needed is to include a new subroutine for the evaluation of the contribution to the total intermolecular energy due to the LRCs (at the beginning of the simulation), and an additional subroutine for calculating the contribution to the intermolecular energy of a given particle due to the LRCs (each time a molecule is attempted to be moved).

III. MODEL AND SIMULATION DETAILS

We consider chain molecules formed by m identical LJ sites (monomer segments) characterized by a diameter σ and dispersive energy ϵ. The molecules are modeled as linear and rigid with monomer-monomer bond length $L = \sigma$, which means that chains are formed by tangent monomers or segments. The interaction potential between two different molecules is given by

$$u^{LJ}(1,2) = \sum_{i=1}^{m}\sum_{j=1}^{m} 4\epsilon\left[\left(\frac{\sigma}{r_{ij}}\right)^{12} - \left(\frac{\sigma}{r_{ij}}\right)^{6}\right], \quad (22)$$

where r_{ij} is the distance between monomer i of molecule 1 and monomer j of molecule 2. Since we are considering a rigid model the intramolecular potential energy is constant, and we set it to zero. As in a previous work,[36] the internal energies reported here are due only to intermolecular interactions (and not intramolecular interactions). As previously discussed in the Introduction, it is important to distinguish between this model and a similar one, the fully-flexible model. In this latter system, molecules are flexible, i.e., there is no restriction neither for the bonding or the torsional angles), so that each monomer of a certain chain interacts with all other monomers in the system (in the same molecule or in other molecules with the only exception of the monomer(s) to which it is bonded) with the Lennard-Jones potential. As mentioned previously, in the first model the interactions between segments are identical

to those in the fully-flexible model, but as the chains are rigid, intramolecular interactions (interactions between segments in the same molecule) are now irrelevant since their contribution to the Hamiltonian of the system is simply a constant, as noted before.

We examine a spherically truncated potential model with a cut-off distance of $r_c = 3\sigma$. We consider inhomogeneous LRCs using the MacDowell and Blas[14] recipe (presented in Sec. II), based on the Janeček's method,[27,28] obtaining results for the full LJ potential, i.e., corresponding to infinite truncation distance. According to the discussion of the previous paragraph, since intramolecular interactions are irrelevant for this model, we also set to zero $U_{i,intra}^{\mathrm{LRC}}$ and U_{intra}^{LRC}.

The number of molecules, N, used in each simulation depends on the number of monomers per molecule. We consider $N = 666$, 500, and 400 for systems formed from 3, 4, and 5 monomers, respectively. As in previous studies,[13,14] this choice is made so as to have systems with the same total number of monomers irrespective of the monomers per molecule.

Simulations are performed in the *NVT* ensemble. We consider a system of N molecules at a temperature T in a volume $V = L_x\, L_y\, L_z$, where L_x, L_y, and L_z are the dimensions of the rectangular simulation box. A homogeneous liquid system is first equilibrated in a rectangular simulation box of dimensions $L_x = L_y = 10\sigma$, and $L_z = 24$, 25, and 32σ for systems of rigid-linear LJ chains formed from 3, 4, and 5 monomers, respectively. The box is then expanded to three times its original size along the z direction, while leaving the liquid phase at the center. As a result, we obtain a centered liquid slab with those chain bits spanning across the boundary conditions of the original liquid configuration protruding into empty boxes of equal size at each side. The final overall dimensions of the vapour-liquid-vapour simulation box are therefore $L_x = L_y = 10\sigma$, and $L_z = 72$, 75, and 96σ for the corresponding chain lengths.

The simulations are organized in cycles. A cycle is defined as N trial moves (displacement of the center of mass and/or molecular rotation). The magnitudes of the appropriate displacement and rotations are adjusted so as to get an acceptance rate of 30 % approximately. We use periodic boundary conditions in all three directions of the simulation box.

The calculation of the surface tension is performed using the TA methodology.[9] Since the TA method is a standard and well-known procedure for evaluating the fluid-fluid interfacial tension of a liquid, we only provide the most important features of the technique. For further details we recommend the original work[9] and the most important applications.[10,13,14,16–21,43–45] The implementation of the TA technique involves performing test-area deformations of magnitude ΔA during the course of the simulation at constant N, V, and T every MC cycle. As shown by Gloor *et al.*,[9] the surface tension follows from the computation of the change in Helmholtz free energy associated with the perturbation, which in turn can be expressed as an ensemble average of the corresponding Boltzmann factor. Further details can be found in Ref. 9. We consider in all cases two perturbations of size $\Delta A^* = \Delta A/A_0 = \pm 0.0005$, where $A_0 = L_x L_y = 100\sigma^2$ is the interfacial area of the unperturbed state.

As in previous studies,[13,14] for each length we perform simulations of inhomogeneous systems at different temperatures where vapour-liquid equilibrium is expected. We typically consider either eight or nine temperatures in the range $\sim 0.5\, T_c$ up to $\sim 0.9\, T_c$, where T_c is the critical temperature of the system. Each series is started at an intermediate temperature. This system is well equilibrated for 10^6 MC cycles, and averages are determined over a further period of 2×10^6 MC cycles. The systems at other temperatures of each series are equilibrated for 5×10^5 MC cycles and averages are determined over the same number of cycles (2×10^6). The production stage is divided into M blocks. Normally, each block is equal to 10^5 MC cycles. The ensemble average of the surface tension is given by the arithmetic mean of the block averages and the statistical precision of the sample average is estimated from the standard deviation in the ensemble average from $\overline{\sigma}/\sqrt{M}$, where $\overline{\sigma}$ is the variance of the block averages. We consider $M = 20$, but in some cases averages are taken over more blocks. In particular, in the case of chains formed from five monomeric units ($m = 5$), M is equal to 40. This means that we use 4×10^6 MC cycles for the production stage of each simulation.

All the quantities in our paper are expressed in conventional reduced units, with σ and ϵ being the length and energy scaling units, respectively. Thus, the temperature is given in units of ϵ/k_B, the densities in units of σ^{-3}, the surface tension in units of ϵ/σ^2, and the interfacial thickness in units of σ.

IV. RESULTS AND DISCUSSION

In this section, we present the main results from the simulations of rigid-linear LJ chains with varying chain length. We focus on the interfacial properties, such as density profiles, interfacial thickness, and surface tension of chains considering a cut-off distance of $r_c = 3\sigma$ and the effective LRCs presented in Sec. II. In particular, we examine the temperature and chain length dependence of these properties.

We follow the same analysis and methodology than in our previous works,[13,14] and consider different chain lengths and temperatures. The equilibrium density profiles $\rho(z)$ are computed from averages of the histogram of densities along the z direction over the production stage. For convenience, density profiles are presented in terms of the monomeric units. The bulk vapour and liquid densities are obtained by averaging $\rho(z)$ over appropriate regions sufficiently removed from the interfacial region. This procedure is meaningful as far as the central liquid slab is thick enough. This turns out to be the case in our simulations, including those performed at the higher temperatures. The bulk vapour density is obtained after averaging the density profiles on both sides of the liquid film. The statistical uncertainty of these values is estimated from the standard deviation of the mean values. Following our previous works, additional interfacial properties, such as the position of the Gibbs-dividing surface, z_0, and the 10−90 interfacial thickness, t, are obtained by fitting each of the two equilibrium density profiles to hyperbolic tangent functions[1] (see Eq. (3) of our previous work[13] for further details). We fix liquid, ρ_L, and vapour, ρ_V, densities to previously computed values and treat z_0 and t as adjustable parameters.

TABLE I. Liquid density ρ_L, vapour density ρ_V, 10−90 interfacial thickness t, and surface tension γ at different temperatures for systems of rigid-linear LJ chains formed from m monomers with a monomer-monomer LJ cut-off distance $r_c = 3\sigma$ and inhomogeneous LRCs. All quantities are expressed in the reduced units defined in Sec. III. The errors are estimated as explained in the text.

m	T	ρ_L	ρ_V	t	γ
3	1.10	0.826(3)	0.00010(6)	1.919(8)	1.07(2)
3	1.20	0.794(2)	0.0009(2)	2.155(5)	0.92(2)
3	1.30	0.763(2)	0.0022(3)	2.447(7)	0.78(1)
3	1.40	0.730(2)	0.0035(2)	2.77(1)	0.69(1)
3	1.50	0.696(1)	0.0073(4)	3.18(1)	0.55(1)
3	1.60	0.660(1)	0.0155(5)	3.689(5)	0.437(7)
3	1.70	0.619(1)	0.0269(4)	4.33(6)	0.331(8)
3	1.80	0.576(1)	0.0413(7)	5.38(6)	0.228(6)
3	1.85	0.548(2)	0.0501(2)	6.02(4)	0.195(6)
4	1.45	0.765(3)	0.0006(1)	2.54(1)	0.77(2)
4	1.50	0.747(2)	0.0009(2)	2.691(5)	0.72(2)
4	1.60	0.712(2)	0.0035(2)	2.99(3)	0.60(1)
4	1.70	0.679(2)	0.0067(3)	3.44(1)	0.50(1)
4	1.80	0.641(2)	0.0107(2)	3.96(6)	0.40(1)
4	1.85	0.623(2)	0.0159(4)	4.27(8)	0.362(9)
4	1.90	0.601(2)	0.0226(7)	4.53(4)	0.30(1)
4	1.95	0.584(1)	0.0272(4)	5.049(9)	0.263(9)
5	2.05	0.611(2)	0.0158(6)	4.78(1)	0.31(5)
5	2.10	0.588(2)	0.0200(5)	5.22(6)	0.27(5)
5	2.15	0.565(3)	0.0258(5)	5.89(3)	0.26(2)
5	2.20	0.546(2)	0.0321(8)	6.6(2)	0.21(1)
5	2.23	0.525(2)	0.037(1)	6.96(4)	0.17(2)
5	2.25	0.519(2)	0.0414(9)	7.6(3)	0.154(9)
5	2.27	0.502(3)	0.046(2)	7.9(4)	0.13(1)
5	2.30	0.490(2)	0.0522(4)	9.0(8)	0.12(1)

Our simulation results for the bulk densities and interfacial thickness for rigid-linear LJ chains formed from 3, 4, and 5 monomers are collected in Table I. The interfacial thickness values summarised here correspond to the average of the values for the two interfaces appearing in the system.

We show in Fig. 1 the segment density profiles $\rho(z)$ for rigid-linear LJ chains formed from three, four, and five monomers ($m = 3$, 4, and 5) at several temperatures in the vapour-liquid coexistence region. For the sake of clarity, we only present one half of the profiles corresponding to one of the interfaces. Also for convenience, all density profiles have been shifted along z so as to place z_0 at the origin. As can be seen, the slope (in absolute value) of the density profiles in the interfacial region decreases as the temperature is increased, an obvious behaviour since the system approaches the critical point, where the interfacial thickness must diverge. A less obvious but also expected decreasing behaviour can be noticed in the slope of the profiles when going from the vapour to the liquid phase, at constant temperature, as the chain length is increased from $m = 3$ (Fig. 1(a)), through $m = 4$ (Fig. 1(b)), and finally up to $m = 5$ (Fig. 1(c)). This is in agreement with the increase of the surface tension as the chain length increases (at constant temperature), as we will show later in this work.

It is important to mention in this context that the density profiles corresponding to chains formed from five monomers were significantly more difficult to equilibrate than the corresponding to chains formed from three and four monomeric units. This is certainly clear when comparing the number of Monte Carlo cycles needed for equilibrating them. In the case of the shorter chains ($m = 3$ and 4), only 2×10^6 cycles were necessary for obtaining well equilibrated density profiles and smooth values of the surface tension along the vapour-liquid coexistence region. As previously mentioned, longer simulations were needed to equilibrate the system formed from five monomeric units ($m = 5$). We think this is due probably to the

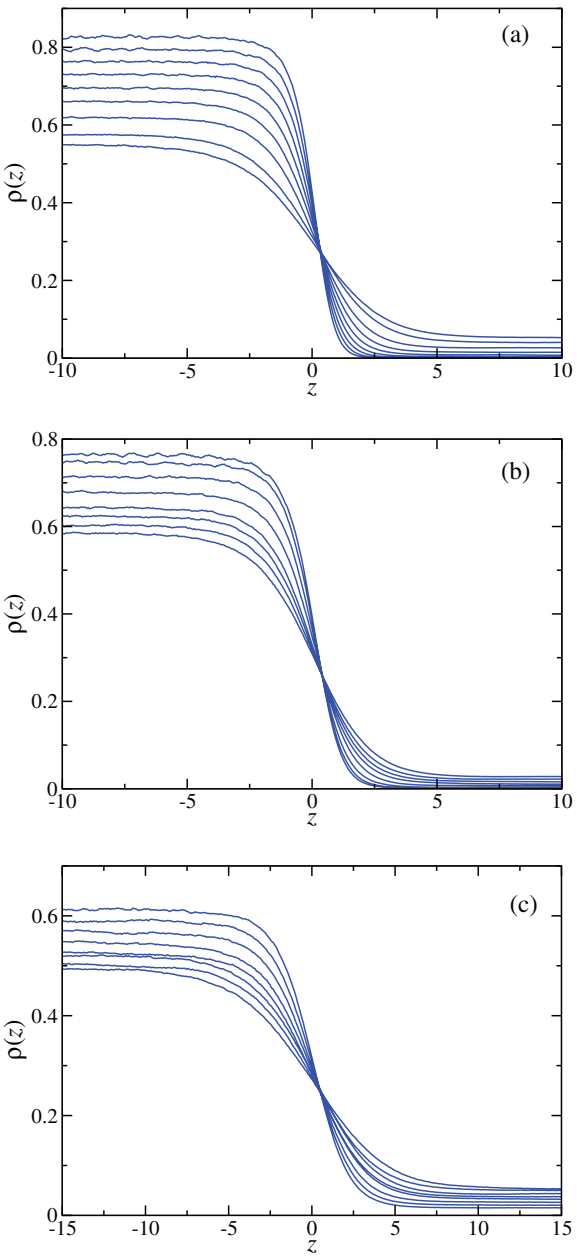

FIG. 1. Simulated equilibrium density profiles across the vapour-liquid interface of rigid-linear LJ chains formed from three ($m = 3$), four ($m = 4$), and five ($m = 5$) monomers with a monomer-monomer LJ cutoff of $r_c = 3\sigma$ and inhomogeneous LRCs at several temperatures. From top to bottom (in the liquid region): (a) $T = 1.10$, 1.20, 1.30, 1.40, 1.50, 1.60, 1.70.1.80, and 1.85; (b) $T = 1.45$, 1.50, 1.60, 1.70, 1.80, 1.85, 1.90, and 1.95; (c) $T = 2.05$, 2.10, 2.15, 2.20, 2.23, 2.25, 2.27, and 2.30.

TABLE II. Critical temperature and density from the analysis of the coexistence densities. All quantities are expressed in the reduced units defined in Sec. III.

m	ρ_c^a	T_c^a	ρ_c^b	T_c^b	T_c^c
3	0.27(1)	2.05(2)	0.27(1)	2.08(2)	2.1(2)
4	0.26(1)	2.25(3)	...	...	2.3(3)
5	0.24(2)	2.50(4)	0.23(5)	2.49(6)	2.6(2)

[a]Using Eqs. (23) and (24).
[b]Taken from the work of Galindo *et al.*[36]
[c]Critical temperature obtained from the analysis of the computed tension data using Eq. (25) and fixing the critical point to $\mu = 1.258$.

increasing stability of a nematic phase, relative to the isotropic liquid, as the chain length is increased. According to preliminary studies of Blas and del Río,[38] simulations for rigid-linear LJ chains formed from seven ($m = 7$) and eight ($m = 8$) segment units indicate that these systems exhibit stable nematic phase between isotropic liquid and solid phases. However, it is important to notice that no stable nematic neither other liquid crystal phase has been found for $m = 5$.

It is also useful to estimate the location of the critical point resulting from our direct Monte Carlo simulations. The critical temperature T_c and density ρ_c are obtained using the simulation results for the vapour and liquid coexistence densities (Table I) and the scaling relation for the width of the coexistence curve,

$$\rho_L - \rho_V = A(T - T_c)^\beta, \tag{23}$$

and the law of rectilinear diameters

$$\frac{\rho_L + \rho_V}{2} = B + CT. \tag{24}$$

A, B, and C are constants, and β is the corresponding critical exponent. A universal value of $\beta = 0.325$ is assumed here.[1] In Table II we report the values of the critical temperatures and densities as obtained from this procedure for all the systems studied in this work.

The vapour-liquid phase envelopes of rigid-linear LJ chains with $r_c = 3\sigma$ and inhomogeneous LRCs are depicted in Fig. 2. As previously mentioned, densities are presented in terms of the monomeric densities since the coexistence curves fall in the same scale when plotted in this way. As can be seen, the phase envelope becomes wider as the chain length is increased, as one would expect. A similar behaviour is also observed for the critical temperature. In order to check the consistency of our results, as well as the expressions proposed in Sec. II for the inhomogeneous LRCs for rigid-linear LJ chains, we have compared the predictions obtained from *NVT* MC simulations of this work with previous results obtained by some of us several years ago[36] using Gibbs ensemble Monte Carlo method and by performing isobaric-isothermal *NPT* calculations at zero pressure. As can be seen in Fig. 2, results obtained from both methods are in excellent agreement at all the temperatures considered. This comparison is obviously a convincing test for consistency for the inhomogeneous LRCs. Note that similar consistent results have been found in previous applications of the method.[14] In addition to that, Fig. 2 also shows a good agreement between critical temperatures and densities obtained here and those calculated by

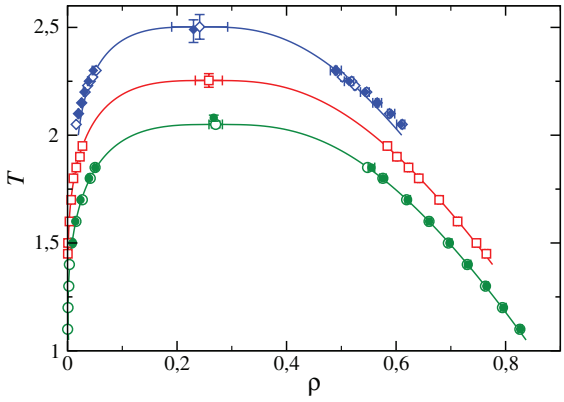

FIG. 2. Vapour-liquid coexistence densities for rigid-linear LJ chains with a monomer-monomer LJ cut-off distance of $r_c = 3\sigma$ and inhomogeneous LRCs. The open green circles, red squares, and blue diamonds correspond to the coexistence densities obtained from the analysis of the equilibrium density profiles obtained from MC *NVT* simulations for chain lengths of $m = 3$, 4, and 5, respectively. The filled green circles and blue diamonds correspond to the coexistence densities obtained from Gibbs ensemble MC and by performing isobaric-isothermal *NPT* calculations at zero pressure by Galindo *et al.*[36] Symbols at the highest temperatures for each of the coexistence curve represent critical points estimated from Eqs. (23) and (24) and those taken from the work by Galindo *et al.*[36]

Galindo *et al.*[36] Critical data obtained from simulation in this work from vapour-liquid coexistence data and surface tension analysis, as well as the values obtained from previous Gibbs ensemble Monte Carlo data[36] are presented in Table II.

Another interesting property obtained from our analysis is the 10−90 interfacial thickness (cf. Table I). For a given chain length, t is seen to increase with temperature, which simply reflects the fact that the interfacial region gets correspondingly wider, as can be observed in Fig. 2. At low temperatures the density profiles exhibit a sharp interface, which corresponds to a low value of the interfacial thickness. As the temperature is increased towards the critical value, the interfacial region becomes wider, and hence, the value of the interfacial thickness increases and diverges to infinity as $T \to T_c$. The variation of interfacial thickness with temperature for different chain lengths is illustrated in Fig. 3. According to the figure, increasing the chain length results in a decrease of the thickness of the interface at fixed temperature, which is consistent with the fact that the systems of longer molecules have a larger cohesive energy. This behavior is consistent with that found for the shape of the vapour-liquid phase envelopes. The behaviour observed here is similar to that predicted previously for the case of fully-flexible LJ chains obtained by Blas *et al.*[13] and MacDowell and Blas.[14] The main difference between both results, as explained previously in the Introduction, is the range of temperatures at which vapour-liquid phase equilibria is stable in both models: whereas the fully-flexible LJ chain model exhibits a huge range in which vapour and liquid phases coexist, the vapour-liquid coexistence range corresponding to the rigid-linear chain model is much more limited.[36] Another subtle difference between both models is the fluctuation of the interfacial width. The values of the error bars of the interfacial thickness corresponding to the shortest chains lengths studied here, $m = 3$ and 4, are

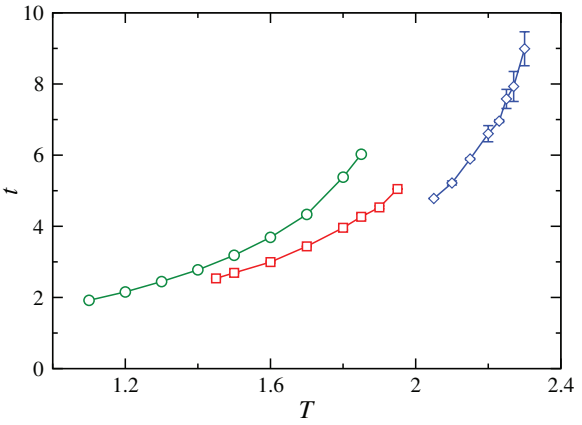

FIG. 3. The 10−90 interfacial thickness t as a function of the temperature for rigid-linear LJ chains with a monomer-monomer cut-off distance of $r_c = 3\sigma$ and inhomogeneous LRCs. The meaning of the symbols is the same as in Fig. 2. The curves are included as a guide to the eyes.

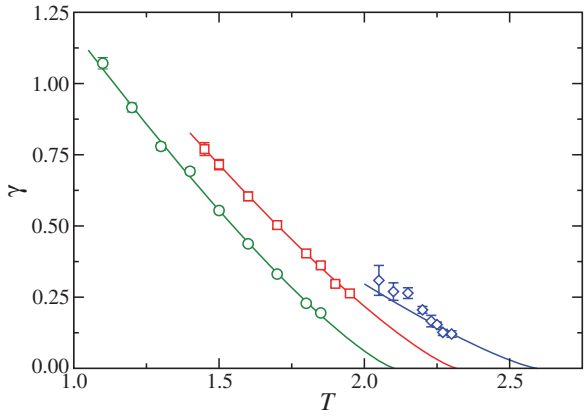

FIG. 4. Surface tension as a function of the temperature for rigid-linear LJ chains with a monomer-monomer LJ cut-off distance of $r_c = 3\sigma$ and inhomogeneous LRCs calculated using the TA methodology. The meaning of the symbols is the same as in Fig. 2. The curves represent the fits of the simulation data to the scaling relationship of the surface tension near the critical point given by Eq. (25) with $\mu = 1.258$.

similar to those obtained for fully-flexible LJ chains with the same size.[13,14] However, relatively larger values have been obtained for the interfacial width corresponding to the longest chain length studied in this work. As previously mentioned in this section, we think this phenomenon is associated to the relative instability of the isotropic liquid phase with respect to a liquid crystalline phase (possibly nematic), and the corresponding fluctuations of the interface.

The density profiles of chains with five monomers (see Fig. 1) show systematically more fluctuations than those corresponding to chains formed from three and four monomeric segments, especially in their corresponding bulk (liquid and vapour) regions. Particularly, equilibrium density profiles for chains form from three and four LJ segments were equilibrated during 2×10^6 cycles, whereas for chains with five segments 4×10^6 cycles were needed in order to have similar equilibrated density profiles. In order to check if the fluctuations found in the case of the longest chains are due to the hypothetical nematic fluctuations in the system, we have also determined the nematic order parameter profile along the vapour-liquid interface for all the chains lengths and at several temperatures. Our results indicate that the order parameter is equal to zero in both phases, vapour and liquid, for all the chainlengths considered and at all temperatures considered. However, larger fluctuations but still negligible, where found in the case of the longest chain-like molecules considered ($m = 5$) in comparison with those for chains with $m = 3$ and 4. Finally, as mentioned previously here, Blas and del Río[38] have found that systems formed from longer chain lengths, i.e., $m = 7$ and 8, exhibit stable nematic phases at certain thermodynamic conditions, another result suggesting that the vapour- (isotropic) liquid coexistence will become unstable if the chain length is increased.

The temperature dependence of the surface tension for rigid-linear LJ chains is shown in Fig. 4. At any given temperature, the interfacial tension is larger for longer chains. Once again, this is consistent with the larger cohesive energy in systems consisting of long chains. As can be seen from Fig. 4, an essentially linear behavior is found for the range of temperatures considered here, with a slight curvature close to the critical point for each system. The effect of chain length on the slope of the surface tension curves is remarkable. At a given temperature, this slope becomes less negative as m is increased, a trend which is also exhibited by fully-flexible LJ chains,[13,14] as well as by the first members of the n-alkane series.[46] The same qualitative behavior has been previously found by Bryk and collaborators.[47]

The computed values of the surface tension allow us to obtain an independent estimate of the critical temperature for each chain length from the scaling relation

$$\gamma = \gamma_0 (1 - T/T_c)^{\mu}, \tag{25}$$

where γ is the surface tension at temperature T, γ_0 is the "zero-temperature" surface tension, μ is the corresponding critical exponent, and T_c is the critical temperature. Here, we fix μ to the universal value of $\mu = 1.258$ as obtained from renormalization group theory (RGT).[1] Our estimates for the critical temperatures are collected in Table II. The overall agreement between these values and those obtained from an analysis of the coexistence densities is satisfactory. It is also possible to compare these results with predictions obtained previously by Galindo *et al.*[36] using Gibbs ensemble Monte Carlo data. As can be seen in Table II, the agreement between both results is satisfactory in all cases.

Similar to the case of fully-flexible LJ chains, the rigid-linear model seems to exhibit a certain convergence of the surface tension with increasing the chain length; however, as we have previously mentioned in this work, the asymptotic regime is not possible to attain for this model due to the presence of the solid phase, which turns out to be more stable than the liquid at the corresponding thermodynamic conditions as it was demonstrated by Galindo *et al.*[36] several years ago. Nevertheless, and following the corresponding-states principle of Guggenheim,[48] as noticed recently by Galliero,[15] we have demonstrated that it is possible to provide a universal scaling behaviour for the vapour-liquid surface tension

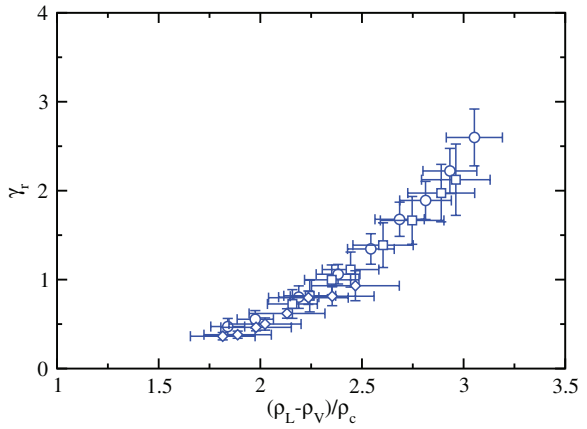

FIG. 5. Reduced surface tension as a function of the difference between the vapour and liquid coexistence densities with respect to the critical density for rigid-linear LJ chains with a monomer-monomer LJ cut-off distance of $r_c = 3\sigma$ and inhomogeneous LRCs. The blue circles, blue squares, and blue diamonds correspond to the reduced surface tension is calculated according to Eq. (26).

of several molecular chain-like systems using the appropriate reduced units and representing the corresponding values as a function of the difference between liquid and vapour densities relative to the critical density.[49] Following previous works,[15,48,50] the vapour-liquid surface tension is reduced as

$$\gamma_r = \frac{\gamma}{k_B T_c (\rho_c/m)^{2/3}}, \tag{26}$$

where k_B is Boltzmann constant, ρ_c and T_c are the critical density and temperature, and m is the chain length of the system. The key point here is to represent γ_r, not as a function of the temperature T or the usual reduced temperature used in the literature, i.e., T/T_c, but in terms of the difference between the vapour and liquid densities. This way of expressing the surface tension closely follows the spirit of the Macleod's parachord approach. Although this simple but successful correlation is clearly empirical, its functional expression can be founded in the more fundamental and modern RGT, as recently shown by Blas and co-workers.[50] According to this, Fig. 5 shows the reduced surface tension of rigid-linear LJ chains formed from three, four, and five segments. As can be seen, a universal behaviour is observed for all the systems considered here, showing that the relationship given by Eq. (26) is also valid for rigid molecular systems.

V. CONCLUSION

We have determined the interfacial properties of the vapour-liquid interface of rigid-linear chains formed by tangentially bonded LJ monomers. Chains formed from three, four, and five monomers are considered. The intermolecular monomer-monomer interactions are truncated at a cut-off distance of 3σ, σ being the diameter of the monomers. In addition, we use an improved version of the Janeček methodology proposed recently by MacDowell and Blas that allows to evaluate the long-range corrections to the potential energy as an effective pairwise intermolecular potential, without need of the explicit calculation of the current density profile along the simulation. We use Monte Carlo *NVT* simulations of the inhomogeneous system containing two vapour-liquid interfaces. The surface tension is evaluated using the TA approach. We have examined the density profiles, interfacial thickness, and surface tension in terms of the temperature and the number of monomers forming the chains. In addition, we have also calculated the coexistence phase envelope, including the location of the critical point from an analysis of the density profiles and the surface tension.

The effect of the chain length on the density profiles, coexistence densities, critical temperature and density, interfacial thickness, and surface tension has been investigated. The vapour-liquid interface is seen to sharpen with increasing chain length corresponding to an increase in the width of the coexistence phase envelope, and an accompanying increase in the surface tension. The vapour-liquid surface tension of rigid-linear LJ chains is seen to exhibit a universal scaling behaviour when is appropriately reduced with respect to the chain length and critical density and temperature, and represented as a function of the difference between the vapour and liquid coexistence densities (relative to the critical point).

ACKNOWLEDGMENTS

The authors would like to acknowledge helpful discussions with F. J. Martínez-Ruiz, E. de Miguel, C. Vega, and A. Galindo. This work was supported by Ministerio de Ciencia e Innovación (MICINN, Spain) through Grant Nos. FIS2010-14866 (F.J.B.), FIS2009-07923 (J.M.M. and M.M.P.) and FIS2010-22047-C05-05 (L.G.M.D.). J.M.M. also acknowledges Ministerio de Ciencia e Innovación for the FPU Grant with reference AP2007-02172. Further financial support from Proyecto de Excelencia from Junta de Andalucía (Grant No. P07-FQM02884), Consellería de Educacion e Ordenacion Universitaria (Xunta de Galicia), Comunidad Autónoma de Madrid (Grant No. MODELICO-P2009/EPS-1691), and Universidad de Huelva are also acknowledged.

[1] J. S. Rowlinson and B. Widom, *Molecular Theory of Capillarity* (Claredon, 1982).
[2] D. Henderson, *Fundamentals of Inhomogeneous Fluids* (Dekker, New York, 1992).
[3] H. T. Davis, *Statistical Mechanics of Phases, Interfaces, and Thin Films* (VCH, Weinheim, 1996).
[4] J. H. Irving and J. G. Kirkwood, J. Chem. Phys. **18**, 817 (1950).
[5] A. Harasima, Adv. Chem. Phys. **1**, 203 (1958).
[6] F. Varnik, J. Baschnagel, and K. Binder, J. Chem. Phys. **113**, 4444 (2000).
[7] E. de Miguel, J. Phys. Chem. B **112**, 4647 (2008).
[8] L. G. MacDowell and P. Bryk, Phys. Rev. E **75**, 061609 (2007).
[9] G. J. Gloor, G. Jackson, F. J. Blas, and E. de Miguel, J. Chem. Phys. **123**, 134703 (2005).
[10] E. de Miguel and G. Jackson, J. Chem. Phys. **125**, 164109 (2006).
[11] E. de Miguel and G. Jackson, Mol. Phys. **104**, 3717 (2006).
[12] P. E. Brumby, A. J. Haslam, E. de Miguel, and G. Jackson, Mol. Phys. **109**, 169 (2011).
[13] F. J. Blas, L. G. MacDowell, E. de Miguel, and G. Jackson, J. Chem. Phys. **129**, 144703 (2008).
[14] L. G. MacDowell and F. J. Blas, J. Chem. Phys. **131**, 074705 (2009).
[15] G. Galliero, J. Chem. Phys. **133**, 074795 (2010).
[16] C. Vega and E. de Miguel, J. Chem. Phys. **126**, 154707 (2007).
[17] J. M. Míguez, D. González-Salgado, J. L. Legido, and M. M. Piñeiro, J. Chem. Phys. **132**, 184102 (2010).

[18]G. Galliero, M. M. Piñeiro, B. Mendiboure, C. Miqueu, T. Lafitte, and D. Bessières, J. Chem. Phys. **130**, 104704 (2009).
[19]E. de Miguel, N. G. Almarza, and G. Jackson, J. Chem. Phys. **127**, 034707 (2007).
[20]C. Miqueu, J. M. Míguez, M. M. Piñeiro, T. Lafitte, and B. Mendiboure, J. Phys. Chem. B **115**, 9618 (2011).
[21]F. Biscay, A. Ghoufi, V. Lachet, and P. Malfreyt, J. Chem. Phys. **131**, 124707 (2009).
[22]E. M. Blokhius, D. Bedeaux, C. D. Holcomb, and J. A. Zollweg, Mol. Phys. **15**, 665 (1995).
[23]M. Mecke, J. Winkelmann, and J. Fischer, J. Chem. Phys. **107**, 9264 (1997).
[24]M. Mecke, J. Winkelmann, and J. Fischer, J. Chem. Phys. **110**, 1188 (1999).
[25]K. C. Daoulas, V. A. Harmandaris, and V. G. Mavrantzas, Macromolecules **38**, 5780 (2005).
[26]M. Guo and B. C.-Y. Lu, J. Chem. Phys. **106**, 3688 (1997).
[27]J. Janeček, J. Phys. Chem. B **110**, 6264–6269 (2006).
[28]J. Janeček, H. Krienke, and G. Schmeer, J. Phys. Chem. B **110**, 6916–6923 (2006).
[29]R. de Gregorio, J. Benet, N. A. Katcho, F. J. Blas, and L. G. MacDowell, J. Chem. Phys. **136**, 104703 (2012).
[30]M. P. Allen, *Computer Simulation of Liquids* (Claredon, Oxford, 1987).
[31]D. Frenkel and B. Smit, *Understanding Molecular Simulations*, 2nd ed. (Academic, San Diego, 2002).
[32]Y.-J. Sheng, A. Z. Panagitopoulos, S. K. Kumar, and I. Szleifer, Macromolecules **27**, 400 (1994).
[33]Y.-J. Sheng, A. Z. Panagitopoulos, and S. K. Kumar, Macromolecules **29**, 4444 (1996).
[34]F. Escobedo and J. J. de Pablo, Mol. Phys. **87**, 347 (1996).
[35]D. Duque, J. C. Pàmies, and L. F. Vega, J. Chem. Phys. **121**, 11395 (2004).
[36]A. Galindo, C. Vega, E. Sanz, L. G. MacDowell, E. de Miguel, and F. J. Blas, J. Chem. Phys. **120**, 3957 (2004).
[37]C. Vega, C. McBride, and L. G. MacDowell, J. Chem. Phys. **115**, 4203 (2001).
[38]F. J. Blas and E. M. del Río, private communication (2012).
[39]B. Smit, S. Karaborni, and J. I. Siepmann, J. Chem. Phys. **102**, 2126 (1995).
[40]B. Smit, Mol. Phys. **85**, 153 (1995).
[41]A. López-Rodríguez, C. Vega, and J. J. Freire, J. Chem. Phys. **111**, 438 (1999).
[42]J. M. Míguez, M. M. Piñeiro, and F. J. Blas, "Influence of the long range corrections to the dispersive potential energy in the calculation of interfacial properties of several molecular models using Monte Carlo simulation," J. Chem. Phys. (unpublished).
[43]F. J. Blas, A. I. M.-V. Bravo, and L. G. MacDowell, "Interfacial properties of Lennard-Jones chains: effect of flexibility" (unpublished).
[44]F. Biscay, A. Ghoufi, F. Goujon, V. Lachet, and P. Malfreyt, J. Chem. Phys. **130**, 184710 (2009).
[45]F. Biscay, A. Ghoufi, F. Goujon, and P. Malfreyt, J. Phys. Chem. B **112**, 13885–13897 (2008).
[46]G. J. Gloor, G. Jackson, F. J. Blas, E. M. del Río, and E. de Miguel, J. Phys. Chem. C **111**, 15513 (2007).
[47]P. Bryk, K. Bucior, S. Sokolowski, and G. Zukocinski, J. Phys.: Condens. Matter **16**, 8861 (2004).
[48]E. A. Guggenheim, J. Chem. Phys. **13**, 253 (1945).
[49]F. J. Blas, L. G. MacDowell, F. J. Martínez-Ruiz, A. I. M.-V. Bravo, and G. Jackson, "Vapor-liquid interfacial properties of square-well chains," J. Chem. Phys. (unpublished).
[50]F. J. Blas, F. J. Martínez-Ruiz, A. I. M.-V. Bravo, and L. G. MacDowell, J. Chem. Phys. **137**, 024702 (2012).